A Study of Unsaturated Pyrazolate-Bridged Diruthenium Carbonyl Complexes

Yi-Hwa Song,[†] Yun Chi,*[,†] Yao-Lun Chen,[†] Chao-Shiuan Liu,*[,†] Wei-Li Ching,[†] Arthur J. Carty,*[,‡] Shie-Ming Peng,[§] and Gene-Hsiang Lee[§]

Department of Chemistry, National Tsing Hua University, Hsinchu 30013, Taiwan, Steacie Institute for Molecular Sciences, National Research Council of Canada, 100 Sussex Drive, Ottawa, Ontario K1A 0R6, Canada, and Department of Chemistry and Instrumentation Center, National Taiwan University, Taipei 10764, Taiwan, Republic of China

Received June 4, 2002

The reaction of $Ru_3(CO)_{12}$ with approximately 3 equiv of 3,5-di-*tert*-butylpyrazole, (dbpz)H, in hexane at 170 °C in a stainless steel autoclave afforded the unsaturated, pyrazolate-bridged diruthenium complex $[Ru_2(CO)_5(dbpz)_2]$ (**2**). The spectroscopic and structural analysis indicated that this compound contains a vacant coordination site at one axial position *trans* to the Ru−Ru linkage. This compound reacted with CO at room temperature to give the saturated complex $[Ru_2(CO)_6(dbpz)_2]$ (**1b**); its structure is analogous to that of the previously determined complexes $[Ru_2(CO)_6(pz)_2]$, pz = pyrazolate and 3,5-dimethyl pyrazolate, except that the equatorial CO ligands show a skew arrangement, an indication of steric constraints within the coordination sphere. Treatment of **2** with benzyl isocyanide or with pyridine in toluene leads to the formation of substitution products $[Ru_2(CO)_4(L)(dbpz)_2]$, L = $CNCH_2Ph$ and pyridine, in which the incoming donor ligand occupies an equatorial position at the saturated Ru center. The structural significance of this pyrazolate-bridged diruthenium complex **2** is discussed.

The chemistry of metal complexes with bridging pyrazolate ligands has attracted great attention because pyrazolate ligands are known to be strongly bond bridging ligands and are capable of holding two metal fragments in close proximity and in chemically stable configurations.[1] Such properties often enhance the cooperative interaction between two metal atoms and are of importance in homogeneous catalysis by bimetallic systems.[2]

Since the first discovery of the diruthenium pyrazolate complexes $[Ru_2(CO)_6(pz)_2]$, pz = pyrazolate and 3,5-dimethylpyrazolate, about a decade ago,[3] relatively few investigations have appeared in the literature, and most of the documented studies deal with fundamental chemical reactions such as oxidations and phosphine substitutions.[4] In contrast, studies of the related carboxylate complexes $[Ru_2(CO)_6(O_2CR)]$, R = Me, Ph, have attracted much more attention because of their latent applications in the catalytic reactions.[5] Apparently, the activity of these bimetallic systems is provided by the generation of a vacant coordination site on one metal at the reaction temperature, which allows the organic substrate to interact with the metal center and initiate the catalytic cycle. Coincident with this result, it was reported that the carboxylate complexes $[Ru_2(CO)_6(\mu\text{-}O_2CR)_2]$ alone spontaneously form the polymeric compound $[Ru_2(CO)_4(\mu\text{-}O_2CMe)_2]_n$ at ambient temperature[6] and in the presence of Lewis bases afford the corresponding donor-stabilized complexes $[Ru_2(CO)_4(\mu\text{-}O_2CMe)_2(L)_2]$ with L being an N-, P-, and S-donor ligand.[7]

* Corresponding authors.
† National Tsing Hua University.
‡ Steacie Institute for Molecular Sciences.
§ National Taiwan University.

(1) (a) La Monica, G.; Ardizzoia, G. A. *Prog. Inorg. Chem.* **1997**, *46*, 151. (b) Bushnell, G. W.; Fjeldsted, D. O. K.; Stobart, S. R.; Zaworotko, M. J.; Knox, S. A. R.; MacPherson, K. A. *Organometallics* **1985**, *4*, 1107. (c) Ardizzoia, G. A.; La Monica, G.; Maspero, A.; Moret, M.; Masciocchi, N. *Inorg. Chem.* **1997**, *36*, 2321. (d) Tejel, C.; Bordonaba, M.; Ciriano, M. A.; Edwards, A. J.; Clegg, W.; Lahoz, F. J.; Oro, L. A. *Inorg. Chem.* **1999**, *38*, 1108. (e) Barbera, J.; Elduque, A.; Gimenez, R.; Lahoz, F. J.; Lopez, J. A.; Oro, L. A.; Serrano, J. L.; Villacampa, B.; Villalba, J. *Inorg. Chem.* **1999**, *38*, 3085.

(2) (a) Contreras, R.; Valderrama, M.; Orellana, E. M.; Boys, D.; Carmona, D.; Oro, L. A.; Lamata, M. P.; Ferrer, J. *J. Organomet. Chem.* **2000**, *606*, 197. (b) Carmona, D.; Ferrer, J.; Arilla, J. M.; Reyes, J.; Lahoz, F. J.; Elipe, S.; Modrego, J.; Oro, L. A. *Eur. J. Inorg. Chem.* **2000**, 159.

(3) (a) Cabeza, J. A.; Landazuri, C.; Oro, L. A.; Tiripicchio, A.; Tiripicchio-Camellini, M. *J. Organomet. Chem.* **1987**, *322*, C16. (b) Cabeza, J. A.; Fernández-Colinas, J. M. *Coord. Chem. Rev.* **1993**, *126*, 319.

(4) (a) Cabeza, J. A.; Landazuri, C.; Oro, L. A.; Belletti, D.; Tiripicchio, A.; Tiripicchio Camellini, M. *J. Chem. Soc., Dalton Trans.* **1989**, 1093. (b) Neumann, F.; Suess-Fink, G. *J. Organomet. Chem.* **1989**, *367*, 175. (c) Neumann, F.; Stoeckli-Evans, H.; Suess-Fink, G. *J. Organomet. Chem.* **1989**, *379*, 151. (d) Shiu, K.-B.; Lee, W.-M.; Wang, C.-L.; Wang, S.-L.; Liao, F.-L.; Wang, J.-C.; Liou, L.-S.; Peng, S.-M.; Lee, G.-H.; Chiang, M. Y. *Organometallics* **1996**, *15*, 2979.

(5) (a) Frediani, P.; Bianchi, M.; Salvini, A.; Piacenti, F. *J. Chem. Soc., Dalton Trans.* **1990**, 3663. (b) Frediani, P.; Faggi, C.; Salvini, A.; Bianchi, M.; Piacenti, F. *Inorg. Chim. Acta* **1998**, *272*, 141. (c) Funaioli, T.; Fachinetti, G.; Marchetti, F. *Chem. Commun.* **1999**, 2043. (d) Salvini, A.; Frediani, P.; Piacenti, F. *J. Mol. Catal. A* **2000**, *159*, 185.

(6) Crooks, G. R.; Johnson, B. F. G.; Lewis, J.; Williams, I. G. *J. Chem. Soc. (A)* **1969**, 2761.

(7) (a) Schumann, H.; Opitz, J.; Pickardt, J. *J. Organomet. Chem.* **1977**, *128*, 253. (b) Sherlock, S. J.; Cowie, M.; Singleton, E.; Steyn, M. M. de V. *Organometallics* **1988**, *7*, 1663. (c) Hilts, R. W.; Sherlock, S. J.; Cowie, M.; Singleton, E.; Steyn, M. M. d. V. *Inorg. Chem.* **1990**, *29*, 3161. (d) Matteoli, U.; Menchi, G.; Bianchi, M.; Piacenti, F.; Ianelli, S.; Nardelli, M. *J. Organomet. Chem.* **1995**, *498*, 177. (e) Kepert, C. M.; Deacon, G. B.; Spiccia, L.; Fallon, G. D.; Skelton, B. W.; White, A. H. *Dalton* **2000**, 2867.

10.1021/om020445r CCC: $22.00
Publication on Web 10/01/2002

However, for the pyrazolate complexes $[Ru_2(CO)_6(pz)_2]$, none of these reaction patterns have been observed, and this reduced reactivity explains the fact that no catalytic reactions have been reported.

In this study, we wish to report the synthesis and structural characterization of two new pyrazolate complexes, $[Ru_2(CO)_6(dbpz)_2]$ (**1b**) and $[Ru_2(CO)_5(dbpz)_2]$ (**2**), dbpz = 3,5-di-*tert*-butylpyrazolate. The first one is structurally related to the pyrazolate complexes reported in the literature and contains 34 valence electrons, while the second shows a similar metal framework, but with a vacant site at one of the axial positions, and contains only 32 valence electrons. This experimental result provides strong structural and chemical evidence for the reaction intermediate involved in activation of substrates by the diruthenium pyrazolate complexes. We hope that these discoveries will provide an incentive for the further exploration of pyrazolate complexes $[Ru_2(CO)_6(pyrazolate)_2]$ as possible catalysts for organic synthesis.

Experimental Section

General Information and Materials. Mass spectra were obtained on a JEOL SX-102A instrument operating in electron impact (EI) mode or fast atom bombardment (FAB) mode. ^1H and ^{13}C NMR spectra were recorded on Varian Mercury-400 or INOVA-500 instruments; chemical shifts are quoted with respect to the internal standard tetramethylsilane for ^1H and ^{13}C NMR data. Elemental analyses were carried out at the NSC Regional Instrumentation Center at National Cheng Kung University, Tainan, Taiwan. The pyrazole ligand 3,5-di-*tert*-butylpyrazole, (dbpz)H, was prepared according to the method reported in the literature.[8] All reactions were performed in air using anhydrous solvents or solvents treated with an appropriate drying reagent.

Synthesis of Complex 1a. A 160 mL stainless steel autoclave was charged with 0.25 g of (dmpz)H (2.60 mmol), 0.5 g of $Ru_3(CO)_{12}$ (0.78 mmol), and 50 mL of hexane. The autoclave was sealed, and the mixture was heated to 180 °C for 24 h. The hexane solvent was then evaporated under vacuum, giving a light yellow material. Recrystallization from a mixture of CH_2Cl_2 and methanol at room temperature afforded 0.47 g of a light yellow crystalline solid $[Ru_2(CO)_6(dmpz)_2]$ (**1a**, 0.84 mmol, 72%). Its spectral data are identical to that reported in the literature.[9]

Synthesis of Complex 2. A 160 mL stainless steel autoclave was charged with 0.85 g of (dbpz)H (4.7 mmol), 1.0 g of $Ru_3(CO)_{12}$ (1.56 mmol), and 50 mL of hexane. The autoclave was sealed and the mixture heated to 170 °C for 24 h. The hexane solvent was then evaporated under vacuum, and the residue was purified using vacuum sublimation at 110 °C and 50 mTorr, giving 1.18 g of a red-orange complex $[Ru_2(CO)_5(dbpz)_2]$ (**2**, 1.68 mmol, 75%). Single crystals suitable for X-ray diffraction study were obtained by recrystallization from a mixture of CH_2Cl_2 and methanol at room temperature.

Spectral Data of 2. MS (FAB, ^{102}Ru): m/z 673 $(M - CO)^+$. IR (CH_2Cl_2): ν(CO), 2093 (s), 2026 (m), 2012 (s), 1998 (m), 1932 (m) cm^{-1}. ^1H NMR (400 MHz, $CDCl_3$, 294 K): δ 5.87 (s, 2H, CH), 1.39 (s, 18H, Me), 1.26 (s, 18H, Me). ^{13}C NMR (100 MHz, $CDCl_3$, 298 K): δ 200.3 (2C, CO), 196.8 (2C, CO), 176.1 (1C, CO), 161.0 (4C, CN), 100.6 (2C, CH), 32.1 (6C, Me), 31.5 (2C, CMe_3), 31.0 (6C, Me), 30.8 (2C, CMe_3). Anal. Calcd for $C_{27}H_{38}N_4O_5Ru_2$: C, 46.28; N, 8.00; H, 5.47. Found: C, 46.05; N, 7.93; H, 5.46.

Synthesis of Complex 1b. A red-orange solution of $[Ru_2(CO)_5(dbpz)_2]$ (100 mg, 0.143 mmol) in 5 mL of CH_2Cl_2 was first placed in a 10 mL sample vial which was capped with a rubber septum. The vial was purged with a slow stream of carbon monoxide, during which time a yellow solution was rapidly obtained. The solution was then concentrated by passing a relatively fast flow of CO. Addition of MeOH over the top of the concentrated solution resulted in the formation of the yellow crystalline complex $[Ru_2(CO)_6(dbpz)_2]$ (**1b**, 98 mg, 0.134 mmol) in 95% yield.

Spectral Data of 1b. IR (CH_2Cl_2): ν(CO), 2088 (s), 2054 (s), 2011 (s), 1993 (m) cm^{-1}. ^1H NMR (400 MHz, $CDCl_3$, 294 K): δ 5.84 (s, 2H, CH), 1.39 (s, 36H, Me). ^{13}C NMR (100 MHz, $CDCl_3$, 298 K): δ 200.2 (4C, CO), 186.4 (2C, CO), 159.6 (4C, CN), 102.3 (2C, CH), 31.5 (4C, CMe_3), 31.2 (12C, Me).

Synthesis of Complex 3a. The complex $[Ru_2(CO)_5(dbpz)_2]$ (57 mg, 0.081 mmol) was first dissolved in 30 mL of toluene. To this was added dropwise 10 μL of benzyl isocyanide (0.085 mmol) using a microsyringe. The mixture was stirred at room temperature for 5 min, during which time the color changed from red to light yellow. The temperature was then increased to 40 °C, and stirring was continued for 4 h. For the workup, the solvent was first removed in vacuo and the oily residue separated by column chromatography (hexane/CH_2CH_2, 1:1), giving a yellow-orange material. Recrystallization from a mixture of CH_2Cl_2 and methanol at room temperature afforded 45 mg of orange crystalline solid $[Ru_2(CO)_4(CNCH_2Ph)(dbpz)_2]$ (**3a**, 0.057 mmol. 70%).

Spectral Data of 3a. MS (EI, ^{102}Ru): m/z 762, $(M - CO)^+$. IR (CH_2Cl_2): ν(CN), 2202 (m); ν(CO), 2039 (m), 1989 (s), 1973 (m), 1914 (m) cm^{-1}. ^1H NMR (400 MHz, $CDCl_3$, 294 K): δ 7.30−7.28 (m, 3H, C_6H_5), 6.93−6.91 (m, 2H, C_6H_5), 5.90 (s, 1H, $CH_{(pz)}$), 5.80 (s, 1H, $CH_{(pz)}$), 4.90 (d, 1H, $^2J_{HH}$ = 16.6 Hz, CH_2), 4.70 (d, 1H, $^2J_{HH}$ = 16.6 Hz, CH_2), 1.39 (s, 9H, Me), 1.33 (s, 9H, Me), 1.27 (s, 9H, Me), 1.24 (s, 9H, Me). ^{13}C NMR (100 MHz, $CDCl_3$, 298 K): δ 202.6 (1C, CO), 201.7 (1C, CO), 200.7 (1C, CO), 181.3 (1C, CO), 160.6 (2C, $CN_{(pz)}$), 160.4 (2C, $CN_{(pz)}$), 147.7 (1C, CN), 131.6 (1C, C_6H_5), 129.0 (2C, C_6H_5), 128.5 (1C, C_6H_5), 126.7 (2C, C_6H_5), 99.9 (2C, CH), 48.5 (1C, CH_2), 32.3 (3C, Me), 32.2 (3C, Me), 32.1 (1C, CMe_3), 31.5 (1C, CMe_3), 30.9 (6C, Me), 30.8 (1C, CMe_3), 30.7 (1C, CMe_3). Anal. Calcd for $C_{34}H_{45}N_5O_4Ru_2$: C, 51.70; N, 8.87; H, 5.74. Found: C, 51.4; N, 8.65; H, 5.76.

Synthesis of Complex 3b. The complex $[Ru_2(CO)_5(dbpz)_2]$ (100 mg, 0.143 mmol) was first dissolved in 30 mL of toluene. To this was added 57 μL of pyridine (0.72 mmol) using a microsyringe. The mixture was refluxed for 18 h, during which time the color gradually changed from red to orange. The solvent was then removed under vacuum to give an orange material. Recrystallization from a mixture of CH_2Cl_2 and methanol at room temperature afforded 102 mg of orange crystalline solid $[Ru_2(CO)_4(py)(dbpz)_2]$ (**3b**, 0.136 mmol. 95%).

Spectral Data of 3b. MS (EI, ^{102}Ru): m/z 724, $(M - CO)^+$. IR (CH_2Cl_2): ν(CO), 2024 (s), 1981 (s), 1947 (m), 1908 (m) cm^{-1}. ^1H NMR (400 MHz, $CDCl_3$, 294 K): δ 7.58 (t, 1H, $^3J_{HH}$ = 7.6 Hz, $CH_{(py)}$), 7.40 (d, 2H, $^3J_{HH}$ = 5.2 Hz, $CH_{(py)}$), 7.05 (t, 2H, $^3J_{HH}$ = 7.1 Hz, $CH_{(py)}$), 6.04 (s, 1H, $CH_{(pz)}$), 5.72 (s, 1H, $CH_{(pz)}$), 1.43 (s, 9H, Me), 1.41 (s, 9H, Me), 1.24 (s, 9H, Me), 1.22 (s, 9H, Me). ^{13}C NMR (100 MHz, $CDCl_3$, 298 K): δ 206.7 (1C, CO), 202.2 (1C, CO), 201.7 (1C, CO), 184.7 (1C, CO), 161.7 (1C, $CN_{(pz)}$), 161.4 (1C, $CN_{(pz)}$), 161.1 (1C, $CN_{(pz)}$), 160.3 (1C, $CN_{(pz)}$), 155.6 (2C, $CN_{(py)}$), 137.3 (1C, $CH_{(py)}$), 124.9 (2C, $CH_{(py)}$), 101.3 (1C, CH), 100.5 (1C, CH), 32.5 (3C, Me), 32.0 (3C, Me), 31.7 (1C, CMe_3), 31.5 (1C, CMe_3), 31.1 (3C, Me), 31.0 (3C, Me), 30.6 (1C, CMe_3), 30.4 (1C, CMe_3). Anal. Calcd for $C_{31}H_{43}N_5O_4Ru_2$: C, 49.52; N, 9.31; H, 5.76. Found: C, 49.61; N, 9.27; H, 5.81.

Synthesis of Complex 4a. An orange solution of $[Ru_2(CO)_4(CNCH_2Ph)(dbpz)_2]$ (100 mg, 0.122 mmol) in 5 mL of CH_2Cl_2 was first placed in a 10 mL sample vial which was capped with a rubber septum. The vial was purged with a slow stream of carbon monoxide, during which time a yellow solution was

(8) (a) Renn, O.; Vananzi, L. M.; Marteletti, A.; Gramlich, V. *Helv. Chim. Acta* **1995**, *78*, 993. (b) Fernandez-Castano, C.; Foces-Foces, C.; Jagerovic, N.; Elguero, J. *J. Mol. Struct.* **1995**, *355*, 265.

(9) Cabeza, J. A.; Oro, L. A. *Inorg. Synth.* **1997**, *31*, 217.

Table 1. Crystal Data and Structure Refinement Parameters for Complexes 1b, 2, and 3a

	2	**1b**	**3a**
empirical formula	$C_{27}H_{38}N_4O_5Ru_2$	$C_{28}H_{38}N_4O_6Ru_2$	$C_{34}H_{45}N_5O_4Ru_2$
fw	700.75	728.76	789.89
diffractometer	Bruker SMART CCD	Nonius Kappa	Nonius Kappa
temperature	150(1) K	150(1) K	150(1) K
cryst syst	monoclinic	monoclinic	monoclinic
space group	*P*2(1)/*n*	*P*2(1)/*c*	*P*2(1)/*n*
a	9.9430(3) Å	20.1549(2) Å	12.1266(2) Å
b	20.8381(7) Å	19.3637(2) Å	15.8058(3) Å
c	14.8887(5) Å	16.8350(2) Å	18.7928(4) Å
β	95.790(1)°	106.8017(4)	99.1720(8)°
volume, *Z*	3069.10(17) Å^3, 4	6289.77(12) Å^3, 8	3555.97(12) Å^3, 4
density(calcd)	1.517 Mg/m^3	1.539 Mg/m^3	1.475 Mg/m^3
abs coeff	1.024 mm^{-1}	1.005 mm^{-1}	0.892 mm^{-1}
F(000)	1424	2960	1616
cryst size (mm^3)	0.30 × 0.30 × 0.12	0.40 × 0.32 × 0.10	0.30 × 0.25 × 0.17
θ ranges	1.69 to 27.5°	2.10 to 27.50°	1.87 to 27.50°
index ranges	−12 < *h* < 11, −26 < *k* < 27, −18 < *l* < 19	−26 < *h* < 26, −25< *k* < 24, −21 < *l* < 21	−15 < *h* < 15, −20 < *k* < 20, −24 < *l* < 24
no. of reflns collected	24 580	51 149	27 604
no. of ind reflns	7038 [*R*(int) = 0.0366]	14435 [*R*(int) = 0.0399]	8148 [*R*(int) = 0.0533]
no. of data/restraints/params	7038/0/343	14 435/0/722	8148/0/419
goodness-of-fit on F^2	1.064	1.244	1.174
final *R* indices [$I>2\sigma(I)$]	$R_1 = 0.0293$, $wR_2 = 0.0579$	$R_1 = 0.0391$, $wR_2 = 0.0952$	$R_1 = 0.0431$, $wR_2 = 0.0981$
R indices (all data)	$R_1 = 0.0498$, $wR_2 = 0.0611$	$R_1 = 0.0587$, $wR_2 = 0.1169$	$R_1 = 0.0717$, $wR_2 = 0.1158$
largest diff peak and hole	1.800 and −0.303 e·Å^{-3}	1.969 and −1.916 e·Å^{-3}	1.260 and −1.068 e·Å^{-3}

obtained. The solution was then concentrated by passing a fast flow of CO. The IR and ^{1}H and ^{13}C NMR analysis showed quantitative conversion to the addition product $[Ru_2(CO)_5(CNCH_2Ph)(dbpz)_2]$ (**4a**), but the solution was found to revert back to the starting material **3a** within several seconds upon purging with nitrogen.

Spectral Data of 4a. IR (CH_2Cl_2): *ν*(CN), 2186 (m); *ν*(CO), 2058 (s), 2014 (s), 1988 (m), 1978 (m), 1959 (m) cm^{-1}. ^{1}H NMR (400 MHz, $CDCl_3$, 294 K): *δ* 7.30 (m, 3H, C_6H_5), 6.92 (m, 2H, C_6H_5), 5.87 (s, 1H, CH), 5.79 (s, 1H, CH), 4.90 (d, 1H, $^2J_{HH}$ = 16.7 Hz, CH_2), 4.77 (d, 1H, $^2J_{HH}$ = 16.7 Hz, CH_2), 1.42 (s, 18H, Me), 1.37 (s, 9H, Me), 1.26 (s, 9H, Me). ^{13}C NMR (100 MHz, $CDCl_3$, 298 K): *δ* 203.9 (1C, CO), 202.5 (1C, CO), 200.6 (1C, CO), 190.3 (1C, CO), 186.8 (1C, CO), 159.0 (2C, CN), 158.9 (2C, CN), 151.5 (1C, CN), 131.9 (1C, C_6H_5), 129.0 (2C, C_6H_5), 128.4 (1C, C_6H_5), 126.5 (2C, C_6H_5), 101.4 (2C, CH), 48.5 (1C, CH_2), 31.6−30.8 (4C, *C*Me$_3$; 12C, Me).

Synthesis of Complex 4b. An orange solution of $[Ru_2(CO)_4(py)(dbpz)_2]$ (50 mg, 0.067 mmol) in 5 mL of CH_2Cl_2 was first placed in a 10 mL sample vial which was capped with a rubber septum. The vial was purged with a slow stream of CO gas, and a yellow solution was obtained. The solution was then concentrated by purging the solution with a fast flow of carbon monoxide. The ^{1}H and ^{13}C NMR analysis showed quantitative conversion to the expected addition product $[Ru_2(CO)_5(py)(dbpz)_2]$ (**4b**), but the solution was found to revert back to the starting material **3b** within several seconds upon re-purging with nitrogen.

Spectral Data of 4b. ^{1}H NMR (400 MHz, $CDCl_3$, 294 K): *δ* 7.53 (t, 1H, $^3J_{HH}$ = 7.6 Hz, $CH_{(py)}$), 7.40 (d, 2H, $^3J_{HH}$ = 5.2 Hz, $CH_{(py)}$), 7.03 (t, 2H, $^3J_{HH}$ = 7.0 Hz, $CH_{(py)}$), 5.99 (s, 1H, CH), 5.70 (s, 1H, CH), 1.45 (s, 9H, Me), 1.43 (s, 9H, Me), 1.27 (s, 9H, Me), 1.21 (s, 9H, Me). ^{13}C NMR (100 MHz, $CDCl_3$, 298 K): *δ* 210.1 (1C, CO), 203.4 (1C, CO), 202.9 (1C, CO), 188.5 (1C, CO), 186.3 (1C, CO), 161.3 (1C, $CN_{(pz)}$), 160.6 (1C, $CN_{(pz)}$), 160.3 (1C, $CN_{(pz)}$), 159.1 (1C, $CN_{(pz)}$), 155.3 (2C, $CN_{(py)}$), 136.8 (1C, $CH_{(py)}$), 124.9 (2C, $CH_{(py)}$), 102.3 (1C, CH), 101.4 (1C, CH), 31.8−31.1 (m, 4C, *C*Me$_3$; 12C, Me).

X-ray Crystallography. Single-crystal X-ray diffraction data were measured on a Nonius Kappa or a Bruker SMART CCD diffractometer using *λ*(Mo Kα) radiation (*λ* = 0.71073 Å). The data collection was executed using the SMART program. Cell refinement and data reduction were exercised using the SAINT program. The structure was determined using the SHELXTL/PC program and refined using full-matrix least squares. All non-hydrogen atoms were refined anisotropically, whereas hydrogen atoms were placed at the calculated positions and included in the final stage of refinements with fixed parameters. Crystallographic refinement parameters of complexes **2**, **1b**, and **3a** are summarized in Table 1, and the selective bond distances and angles of these complexes are listed in Tables 2−4, respectively.

Table 2. Selected Bond Lengths [Å] and Angles [deg] for Complex 2

Bond Lengths and Angles			
Ru(1)−Ru(2)	2.6513(3)	Ru(1)−C(1)	1.911(3)
Ru(1)−C(2)	1.947(3)	Ru(1)−C(3)	1.908(3)
Ru(2)−C(4)	1.863(3)	Ru(2)−C(5)	1.874(3)
Ru(1)−N(1)	2.146(2)	Ru(1)−N(3)	2.131(2)
Ru(2)−N(2)	2.094(2)	Ru(2)−N(4)	2.109(2)
N(1)−N(2)	1.380(3)	N(3)−N(4)	1.381(3)
∠N(1)−Ru(1)−N(3)	87.75(8)	∠N(2)−Ru(2)−N(4)	87.62(8)
∠Ru(2)−Ru(1)−C(2)	172.95(9)		
Torsional Angles			
C(1)−Ru(1)−Ru(2)−C(4)	0.42(13)	C(3)−Ru(1)−Ru(2)−C(5)	2.25(13)

Results and Discussion

Parent Pyrazolate Complexes. It has been reported that treatment of $RuCl_3 \cdot nH_2O$ with granular zinc in the presence of CO and 3,5-dimethylpyrazole, (dmpz)H, led to the formation of a double pyrazolate-bridged ruthenium complex $[Ru_2(CO)_6(dmpz)_2]$ (**1a**) in 85% yield.[9] Alternatively, the same reaction product can be isolated in comparable yield via heating of a hexane solution of $Ru_3(CO)_{12}$ and (dmpz)H in a stainless steel autoclave (170 °C, 24 h). In this case, the reaction conditions are akin to those used for the synthesis of the diosmium pyrazolate complex $[Os_2(CO)_6(hfpz)_2]$, hfpz = 3,5-bis(trifluoromethyl)pyrazolate, described in the literature.[10] Interestingly, both the literature report and our experimental observation have revealed that complex **1a** does not lose CO even at elevated temperature and under vacuum.

(10) Chi, Y.; Yu, H.-L.; Ching, W.-L.; Liu, C.-S.; Chen, Y.-L.; T.-Y., C.; Peng, S.-M.; Lee, G.-H. *J. Mater. Chem.* **2002**, *12*, 1363.

Table 3. Selected Bond Lengths [Å] and Angles [deg] for Complex 1b

Moelcule 1			
Ru(1)−Ru(2)	2.6810(3)	Ru(1)−C(1)	1.978(3)
Ru(1)−C(2)	1.887(3)	Ru(1)−C(3)	1.893(3)
Ru(2)−C(4)	1.899(3)	Ru(2)−C(5)	1.893(3)
Ru(2)−C(6)	1.965(3)	Ru(1)−N(1)	2.128(2)
Ru(1)−N(3)	2.147(3)	Ru(2)−N(2)	2.153(2)
Ru(2)−N(4)	2.126(2)	N(1)−N(2)	1.374(3)
N(3)−N(4)	1.382(3)		
∠N(1)−Ru(1)−N(3)	87.74(9)	∠N(2)−Ru(2)−N(4)	87.89(9)
∠Ru(2)−Ru(1)−C(1)	171.65(9)	∠Ru(1)−Ru(2)−C(6)	173.41(9)
Torsional Angles			
C(2)−Ru(1)−Ru(2)−C(4)	9.30(14)	C(3)−Ru(1)−Ru(2)−C(5)	9.46(15)
Moelcule 2			
Ru(3)−Ru(4)	2.6758(3)	Ru(3)−C(1A)	1.970(3)
Ru(3)−C(2A)	1.901(3)	Ru(3)−C(3A)	1.905(3)
Ru(4)−C(4A)	1.899(3)	Ru(4)−C(5A)	1.884(3)
Ru(4)−C(6A)	1.979(3)	Ru(3)−N(5)	2.126(2)
Ru(3)−N(7)	2.159(2)	Ru(4)−N(6)	2.153(2)
Ru(4)−N(8)	2.122(2)	N(5)−N(6)	1.380(3)
N(7)−N(8)	1.378(3)		
∠N(5)−Ru(3)−N(7)	86.56(9)	∠N(6)−Ru(4)−N(8)	86.76(9)
∠Ru(4)−Ru(3)−C(1A)	172.15(9)	∠Ru(3)−Ru(4)−C(6A)	171.49(9)
Torsional Angles			
C(2A)−Ru(3)−Ru(4)−C(4A)	18.07(14)	C(3A)−Ru(3)−Ru(4)−C(5A)	19.82(14)

Table 4. Selected Bond Lengths [Å] and Angles [deg] for Complex 3a

Bond Lengths and Angles			
Ru(1)−Ru(2)	2.6444(4)	Ru(1)−C(1)	1.874(4)
Ru(1)−C(2)	1.918(4)	Ru(2)−C(3)	1.859(4)
Ru(2)−C(4)	1.852(4)	Ru(1)−C(5)	1.967(4)
C(5)−N(5)	1.142(4)	N(5)−C(6)	1.427(5)
Ru(1)−N(1)	2.161(3)	Ru(1)−N(3)	2.130(3)
Ru(2)−N(2)	2.098(3)	Ru(2)−N(4)	2.133(3)
N(1)−N(2)	1.382(4)	N(3)−N(4)	1.378(4)
∠N(1)−Ru(1)−N(3)	88.61(11)	∠N(2)−Ru(2)−N(4)	86.92(11)
∠Ru(2)−Ru(1)−C(2)	173.35(10)	∠Ru(1)−C(5)−N(5)	178.3(3)
Torsional Angles			
C(2)−Ru(1)−Ru(2)−C(4)	10.21(17)	C(3)−Ru(2)−Ru(1)−C(5)	9.28(15)

However, during our attempts to synthesize the corresponding di-*tert*-butyl-substituted pyrazolate metal complex $[Ru_2(CO)_6(dbpz)_2]$ (**1b**), using the method of direct treatment of $Ru_3(CO)_{12}$ with 3 equiv of 3,5-di-*tert*-butyl-substituted pyrazole (dbpz)H, we obtained an apparently different, orange-red crystalline material (**2**) in excellent yield, which was then purified by vacuum sublimation, followed by recrystallization from a mixture of CH_2Cl_2 and methanol.

This complex was characterized using routine spectroscopic techniques such as FAB mass, IR, and ^{1}H and ^{13}C NMR spectral methods. The FAB mass spectrum shows a parent peak at $m/z = 673$, corresponding to the species with a composition of $Ru_2(CO)_4(dbpz)_2$, which is two CO ligands less than that expected for the saturated complex **1b**. The IR spectrum exhibits four strong terminal ν(CO) stretching bands at 2093 (m), 2026 (m), 2012 (s), and 1932 (m) cm^{-1}, again distinctively different from that of the dmpz analogue **1a**. Moreover, the ^{1}H NMR shows only one CH signal of the pyrazolate ligand at δ 5.87, together with two *tert*-butyl signals at δ 1.39 and 1.26, indicating that the molecule does not have the expected C_{2v} symmetry. Finally, in addition to the signals of the pyrazolate ligands, three CO signals at δ 200.3, 196.8, and 176.1 with an intensity ratio of 2:2:1 were observed in the ^{13}C NMR spectrum. We concluded that these spectral data are inconsistent with those of the expected complex **1b**, for which the possession of two orthogonal mirror planes in the molecule would produce a highly simplified spectral pattern with only one signal for the *tert*-butyl groups in the ^{1}H NMR spectrum and two CO resonance signals with a 4:2 ratio in the ^{13}C NMR spectrum.

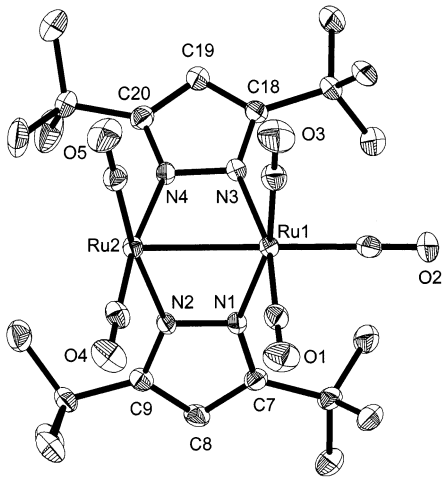

Figure 1. ORTEP drawing of complex **2** with thermal ellipsoids shown at the 50% probability level.

A single-crystal X-ray diffraction study was then carried out to reveal the exact molecular structure. As indicated in Figure 1, the structure of **2** consists of two ruthenium metal atoms bridged by two pyrazolate ligands, which are essentially orthogonal to one another. It is notable that the first ruthenium atom Ru(1) adopts

an octahedral environment consistency of three carbon atoms from terminal carbonyl ligands, two nitrogen atoms from the bridging pyrazolate ligands, and the other ruthenium atom. On the other hand, the second ruthenium atom Ru(2) shows a distinctive, square pyramidal geometry, which is apparently produced by removal of the axial CO ligand at the position opposite the Ru−Ru linkage. The Ru−Ru separation of 2.6513(3) Å is comparable with those found in related binuclear Ru^{I}−Ru^{I} complexes with two bridging ligands, such as $[Ru(\mu\text{-pyO})(CO)_2(pyOH)]_2$, 2.670(1) Å with pyOH = 2-pyridone,[11] $[Ru(\mu\text{-dmpz})(CO)_3]_2$,[2] 2.705(2) Å with dmpz = 3,5-dimethylpyrazolate, and $[Ru(\mu\text{-pz})(CO)_2(PPh_3)]_2$,[12] 2.732(1) Å with pz = pyrazolate, showing a Ru−Ru single-bond bonding interaction.

Moreover, for the octahedral Ru(1) metal center, the Ru−N distances fall in the range 2.146(2)−2.131(2) Å, but the Ru−CO distances exhibit a small variation in bond length (1.991(3)−1.908(3) Å), with the equatorial Ru−CO distance being slightly shorter. Nevertheless, all these metal−ligand distances are significantly longer than those of the respective Ru(2)−N distances to the bridging pyrazolate ligands, 2.109(2) and 2.094(2) Å, and the corresponding Ru−CO distances, i.e., 1.863(3) and 1.874(3) Å, of the Ru(2) metal atom. The shortening of the metal−ligand distances can be attributed to the relief of steric crowding, the lower coordination number of Ru(2) compared to Ru(1), and the strengthening of the ligand to metal σ-donation, required to compensate for the coordination unsaturation at the Ru(2) site. To our knowledge, the only other example of an unsaturated Ru metal center in a binuclear or cluster complex is in the spiked-triangular complex $Ru_4(CO)_9(\mu\text{-}PPh_2)[\mu_4\text{-}Ph_2PCC(Ph)CC(Ph)]$, in which a phenyl group of the PPh_2 fragment partially protects the vacant site but is not directly coordinated.[13]

After establishing the structure of **2**, its reactivity was then examined in an attempt to elucidate whether unique chemical properties were associated with the vacant coordination site. Surprisingly complex **2** did not react with H_2 gas in toluene solution even at elevated temperatures; unreacted starting material was recovered in high yield. This observation suggests that while the vacant coordination site in **2** is incapable of activating dihydrogen, the pyrazolate ligands stabilize the two Ru metal centers to decomposition. However, reaction of **2** with carbon monoxide is instantaneous even at room temperature, and the color of the solution fades away within minutes by purging with CO, indicating the formation of a CO adduct $[Ru_2(CO)_6(dbpz)_2]$ (**1b**). The structure of **1b** was then characterized according to the IR and NMR spectral data and by a single-crystal X-ray diffraction study. To minimize decomposition in solution, a suitable crystal was obtained by layering a CO-saturated MeOH solvent over a concentrated CH_2Cl_2 solution of **2** at room temperature under a CO atmosphere.

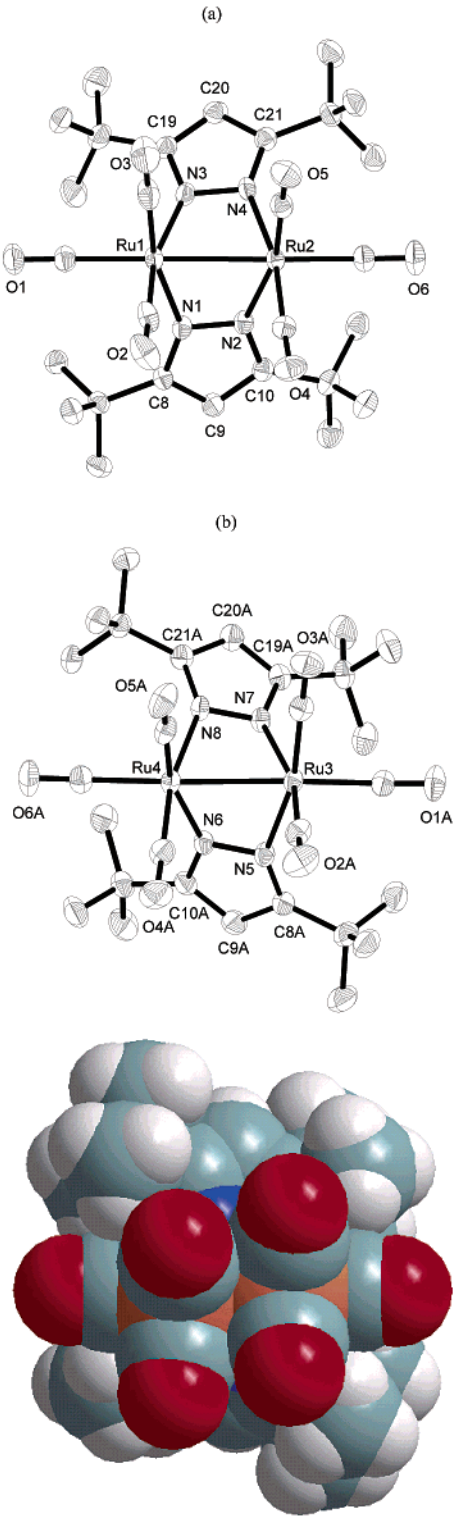

Figure 2. (a) ORTEP drawing of the first molecule of complex **1b** and the corresponding atomic numbering scheme. (b) ORTEP drawing and the respective space-filling plot of the second molecule.

According to the single-crystal X-ray analysis, there are two crystallographically independent molecules within the asymmetric unit. An ORTEP plot of both molecules is depicted in Figure 2, alone with a space-filling plot of the second molecule to show the distortion between the equatorial CO ligands. It is noteworthy that

(11) Andreu, P. L.; Cabeza, J. A.; Carriedo, G. A.; Riera, V.; Garcia-Granda, S.; Van der Maelen, J. F.; Mori, G. *J. Organomet. Chem.* **1991**, *421*, 305.
(12) Sherlock, S. J.; Cowie, M.; Singleton, E.; Steyn, M. M. de V. *J. Organomet. Chem.* **1989**, *361*, 353.
(13) Delgado, E.; Chi, Y.; Wang, W.; Hogarth, G.; Low, P. J.; Enright, G. D.; Peng, S. M.; Lee, G. H.; Carty, A. J. *Organometallics* **1998**, *17*, 2936.

most of the metal−ligand bond lengths and angles in these two molecules are within four standard deviations of each other. However, the first molecule displays a slight skew arrangement (not the expected, staggered arrangement observed in **2**) with an average torsional angle between the equatorial CO ligands being 9.38°, while the second molecule has an even greater skew distortion of 18.5°. A slightly longer metal−metal distance is also observed for the first molecule (Ru(1)−Ru(2) = 2.6810(3) Å) with respect to that of the second molecule (Ru(3)−Ru(4) = 2.6758(3) Å), implying that the torsional angle between the equatorial CO ligands as well as the twisting of the pyrazolate fragments with respect to the Ru−Ru vector is somehow inversely related to the internal Ru−Ru separation.

A close inspection of the relative positions of the axial CO ligands suggests an orientation toward the adjacent *tert*-butyl substituents of the pyrazolate ligands by a very small angle of 6.6−8.3° (∠Ru(2)−Ru(1)−C(1) = 171.65(9)° and ∠Ru(1)−Ru(2)−C(6) = 173.41(9)°). This structural information tends to suggest that there is little physical contact between the axial CO ligands and the adjacent *tert*-butyl substituents of the pyrazolate ligands. However, as mentioned earlier, both pyrazolate fragments are twisted with respect to the Ru−Ru vector, and this motion may in part have reduced excessive steric interaction with the axial CO ligands. If this is the case, it is possible that the poor stability of **1b** with respect to CO elimination may be derived from a need to compensate for steric repulsion between the *tert*-butyl substituents and the axial CO ligands.

For comparison, the space-filling plots of the unsaturated complex **2**, which are viewed from both of the axial directions, are depicted in Figure 3 with all atoms drawn to represent their van der Waals radii. The first space-filling model clearly reveals that there is little steric contact between the axial CO and the *tert*-butyl groups of the pyrazolate ligands at its saturated $Ru(CO)_3$ portion. However, on the opposite side of the molecule, the second set of *tert*-butyl substituents have moved over to the axial, vacant site on the Ru atom and cover at least one-third of the void space above the coordination site. This observation confirms that the dissociation of an axial CO ligand from **1b** must be enhanced by the steric effect of the *tert*-butyl substituents.

Reactions with Donor Ligands. Treatment of a $CDCl_3$ solution of **2** with a stoichiometric amount of benzyl isocyanide led to an immediate color change from red-orange to light yellow after mixing at room temperature. The ^{1}H NMR spectra of this solution indicated the formation of several products, of which the major component displays a sharp singlet at δ 5.02 for the methylene group of the benzyl isocyanide. This observation suggests that the isocyanide donor ligand may have coordinated to the vacant axial site on complex **2** during the initial mixing of the reagents; otherwise, a spectral pattern involving two nonequivalent doublets would be expected. However, this isocyanide complex is rather unstable and undergoes decomposition to several other products upon extending the reaction time, prohibiting the full characterization of this reaction intermediate.

However, on increasing the reaction temperature to 40 °C for 4 h, an isocyanide-substituted complex $[Ru_2(CO)_4(CNCH_2Ph)(dbpz)_2]$ (**3a**) was isolated in 70% yield, after chromatographic separation and recrystallization. Curiously, the ^{1}H NMR spectrum of **3a** exhibits two CH signals at δ 5.90 and 5.80 for the pyrazolate ligands as well as two sets of doublets at δ 4.90 and 4.70 with coupling constant $^2J_{HH}$ = 16.6 Hz. The latter were identified as the diastereotopic methylene hydrogens of the benzyl group. These spectral data imply that the isocyanide ligand has moved to an equatorial position, showing that the mirror symmetry of the previously observed reaction intermediate is no longer retained.

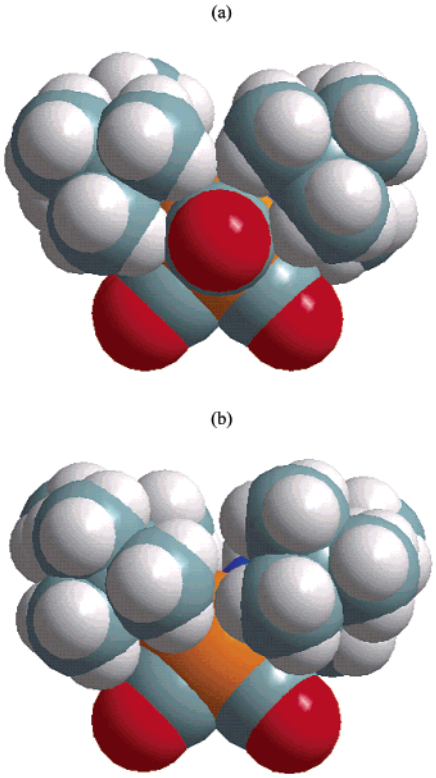

Figure 3. Space-filling plots of complex **2**, showing (a) the steric interaction between the axial CO ligand and the *tert*-butyl substituents and (b) the environment around the vacant coordination site.

The X-ray crystal structure was determined to reveal the exact location of the incoming isocyanide ligand in **3a** (Figure 4). Again, the two Ru atoms are bridged by two dbpz ligands, which are located approximately orthogonal to each other. The Ru−Ru distance, 2.6444(4) Å, is similar to that of **2** and is consistent with the presence of a metal−metal single bond. Moreover, both Ru atoms are coordinated by two carbonyl ligands, while one is further linked to an isocyanide ligand at the equatorial position, and the second possesses the expected vacant axial site. The Ru−C distance to the isocyanide ligand (1.967(4) Å) is slightly shorter than that observed in the isocyanide cluster complex $[Ru_3(CO)_{11}(CNBu^t)]$ (2.040(5) Å), where the metal atoms show a different, zero oxidation state,[14] but is longer than that in the adjacent, equatorial CO ligand of the same molecule (cf. Ru(1)−C(1) = 1.874(4) Å), reflecting the weaker π-accepting properties of the isocyanide. This reduction in the π-acceptor properties is also

(14) Bruce, M. I.; Matison, J. G.; Wallis, R. C.; Patrick, J. M.; Skelton, B. W.; White, A. H. *J. Chem. Soc., Dalton Trans.* **1983**, 2365.

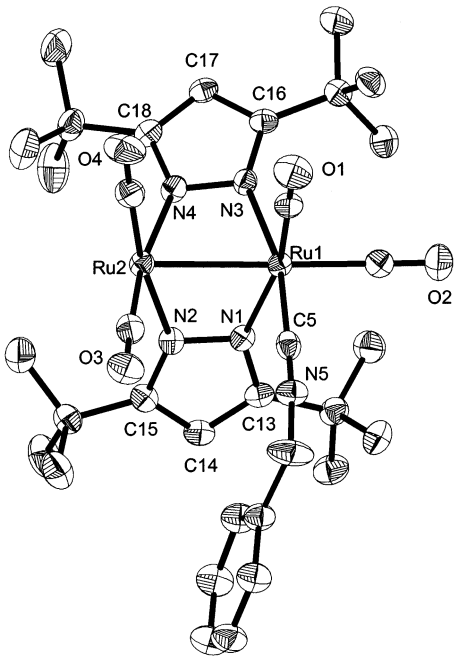

Figure 4. ORTEP drawing of complex **3a** with thermal ellipsoids shown at the 50% probability level.

illustrated by the strengthening of the *trans*-pyrazolate nitrogen atom bonding to the ruthenium atom (Ru(1)−N(3) = 2.130(3) Å). This distance is 0.03 Å shorter than the Ru−N distance to the second pyrazolate (Ru(1)−N(1) = 2.161(3) Å), which is located *trans* to the CO ligand.

The reaction between **2** and a second donor ligand, pyridine, proceeded much slower at room temperature, with no intermediate being observed even under conditions of excess pyridine. However, upon increasing the temperature to 110 °C for 18 h, an orange complex, $[Ru_2(CO)_4(py)(dbpz)_2]$ (**3b**), was isolated in 95% yield. The identification of **3b** was established by ^{13}C NMR spectroscopy, in which four distinctive CO signals at δ 206.7, 202.2, 201.7, and 184.7 are observed, with a spectral pattern nearly identical to that of the related isocyanide complex **3a**, thus allowing the unambiguous confirmation of its molecular structure.

Since both complexes **3a** and **3b** show a similar type of unsaturation with respect to the parent compound **2**, it is reasonable to assume that these substituted complexes would be converted from 32e species to 34e complexes, upon addition of CO gas. Our control experiments have not only confirmed this hypothesis but also showed that the CO-addition products $[Ru_2(CO)_5(L)(dbpz)_2]$ (L = $NCCH_2Ph$, **4a**; L = py, **4b**) are far less stable than the parent complex **1b**, especially in the absence of a CO atmosphere. As a result, although their NMR spectra have been recorded, the instabilities of **4a** and **4b** prohibited measurement of IR ν(CO) spectra due to a rapid reversion to the starting complexes **3a** and **4a** during sample transfer.

Structural Properties. The structural relationship of the complexes **1**−**4** is depicted in Scheme 1. It has been suggested that the methyl derivative **1a** is relatively stable to CO dissociation upon increasing the temperature. However, for the *tert*-butyl-substituted derivative **1b**, a spontaneous decarbonylation reaction occurred at room temperature, giving complex **2** via loss

Scheme 1

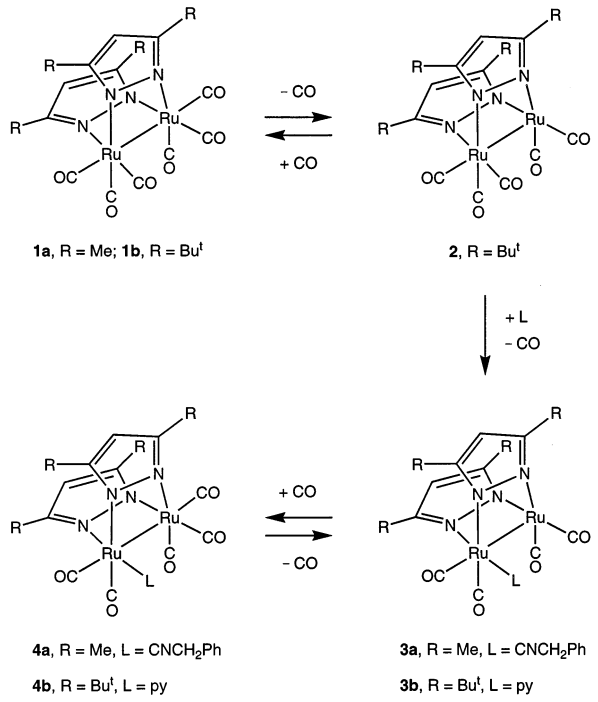

1a, R = Me; **1b**, R = Bu^t **2**, R = Bu^t

4a, R = Me, L = $CNCH_2Ph$ **3a**, R = Me, L = $CNCH_2Ph$

4b, R = Bu^t, L = py **3b**, R = Bu^t, L = py

Scheme 2

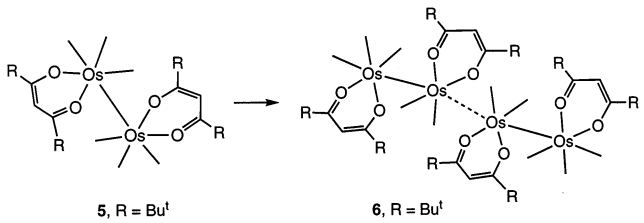

5, R = Bu^t **6**, R = Bu^t

of an axial CO ligand *trans* to the Ru−Ru linkage. This reaction is quantitative in solution, and as a result, the unsaturated complex **2** is the sole product obtained from the direct treatment of $Ru_3(CO)_{12}$ and 3,5-di-*tert*-butylpyrazole, even when a large excess of carbon monoxide is present in the sealed autoclave.

The structure of **1b** is related to that of an isoelectronic complex, $[Os_2(CO)_6(thd)_2]$ (**5**), thd = 2,2-dimethyl-3,5-heptanedionate,[15] for which both of the osmium atoms display an identical d^7 electrical configuration. The only difference is that the thd ligand in **5** is chelated to each osmium atom, rather than serving as a bridging ligand; thus free rotation along the Os−Os vector is possible in the thd complex **5**, producing an eclipsed arrangement for all equatorial ligands. As a result, after the removal of a CO ligand at the axial position, the two $[Os_2(CO)_5(thd)_2]$ units couple to afford the dimer complex $[Os_2(CO)_5(thd)_2]_2$ (**6**), utilizing the so-called double dative interaction[16] to produce a linear Os−Os···Os−Os array (Scheme 2). We speculate that such a process is inaccessible for complex **2** because the *tert*-butyl substituents near the vacant site block the dimerization, and the double pyrazolate bridges within the

(15) Su, M.-D.; Liao, H.-Y.; Chu, S.-Y.; Chi, Y.; Liu, C.-S.; Lee, F.-J.; Peng, S.-M.; Lee, G.-H. *Organometallics* **2000**, *19*, 5400.

(16) (a) Batchelor, R. J.; Davis, H. B.; Einstein, F. W. B.; Pomeroy, R. K. *J. Am. Chem. Soc.* **1990**, *112*, 2036. (b) Wang, W.; Einstein, F. W. B.; Pomeroy, R. K. *Organometallics* **1993**, *12*, 3079. (c) Liu, Y.; Leong, W. K.; Pomeroy, R. K. *Organometallics* **1998**, *17*, 3387.

Ru_2 framework also prevent twisting with respect to the Ru−Ru linkage.

Finally, the IR ν(CO) stretching vibrations of complexes **1a** and **1b** have been utilized to assess the possible contribution from the electronic effect, for which a small, but notable difference in the ν(CO) stretching vibrations (≤ 3 cm^{-1}) was recorded. The low-energy shifting of **1b** indicated that its CO ligands have received an increased amount of back π-bonding from the Ru metal atoms, showing a synergistic effect of the *tert*-butyl substituents in this system.

Summary

The chemical and physical behavior of the parent pyrazolate complexes $[Ru_2(CO)_6(pz)_2]$, pz = pyrazolate ligands, is strongly influenced by the nature of the alkyl substituents on the pyrazolate ligands. Our observation is consistent with a recent report on the monometallic complexes $[Cr(dbpz)_3]$ and $[Fe(dbpz)_3]$,[17] for which the steric bulk of the *tert*-butyl substituents provides the necessary stabilization for the novel η^2-bonding mode. Thus, we are confident that the same steric interaction facilitates CO elimination from the dbpz complex **2**, giving one vacant coordination site at the axial position. Upon addition of benzyl isocyanide, this strong donor ligand coordinates immediately at the vacant coordination site to give an unstable addition product at room temperature, but the addition product was not detected upon switching to the more bulky and less reactive pyridine ligand. Not surprisingly, the reaction is under thermodynamic control, giving a ligand substitution product upon extending the reaction time or increasing the temperature, in which the incoming donor ligand of the substitution products **3a** and **3b** resides at an equatorial site of the saturated Ru metal center. The mechanism leading to this type of substitution product is unclear. From a range of possibilities, we prefer the idea of having sequential addition and elimination, which consists of the initial addition of ligand at the vacant axial site, and then axial-to-equatorial rearrangement, followed by elimination of the second axial CO ligand at the remote Ru atom. Moreover, the progress of this substitution sequence implies that the less π-accepting isocyanide and pyridine ligands have a special tendency to remain at the relatively more electron-rich metal atom, a phenomenon that has no adequate explanation at this moment. Further studies will be aimed at utilizing these congested pyrazolate complexes as catalytic precursors.

Acknowledgment. Y.C. thanks the National Science Council of the Republic of China (NSC 90-2113-M-007-056) and the Chinese Petroleum Corporation, Republic of China, for financial support (CPC 89-2119-M-007).

Supporting Information Available: X-ray crystallographic file for complexes **2**, **1b**, and **3a**. This material is available free of charge via the Internet at http://pubs.acs.org.

OM020445R

(17) Gust, K. R.; Knox, J. E.; Heeg, M. J.; Schlegel, H. B.; Winter, C. H. *Angew. Chem., Int. Ed.* **2002**, *41*, 1591.